


 Cite this: *RSC Adv.*, 2023, **13**, 15667

## Synthesis of bis-spiro piperidines using nano $\gamma$ -alumina supported Sb(v) under ultrasonic irradiation at room temperature conditions†

 Maryam Aghamohammadsadegh,<sup>a</sup> Abdolhamid Bamoniri  <sup>\*a</sup> and Bi Bi Fatemeh Mirjalili  <sup>b</sup>

Group VA metalloid ion Lewis acids, Sb(v) was identified as a highly potent catalyst for the one-pot three-component synthesis of bis-spiro piperidine derivatives. The reaction was performed using amines, formaldehyde, and dimedone under ultrasonic irradiation at room temperature. The strong acidic property of the nano  $\gamma$ -alumina supported antimony(v) chloride plays a key role in accelerating the rate of the reaction and initiates the reaction smoothly. The heterogeneous nanocatalyst was fully characterized by FT-IR spectroscopy, XRD, EDS, TGA, FESEM, TEM, and BET techniques. Also, the structures of the prepared compounds were characterized by  $^1\text{H}$  NMR and FT-IR spectroscopies.

Received 20th January 2023

Accepted 7th May 2023

DOI: 10.1039/d3ra00448a

[rsc.li/rsc-advances](http://rsc.li/rsc-advances)

### 1. Introduction

One-pot multicomponent reactions (MCRs) with high atom economy play an important role in combinatorial chemistry.<sup>1–5</sup> As such, this field has attracted considerable attention in recent years. During MCRs, target compounds are produced with greater efficiency by generating structural complexity in a single step from three or more reactants.<sup>6,7</sup>

It is well known that spiro-fused piperidine represents one of the most pervasive heterocyclic motifs and is present in many naturally occurring alkaloids, animal toxins, biologically active synthetic molecules, and organic fine chemicals.<sup>8–10</sup> The piperidine structure is also present in abundant products, such as piperine (present in black pepper), the nicotine analogue anabasine of tree tobacco (*Nicotiana glauca*), lobeline of Indian tobacco, and the toxic alkaloid coniine from poison hemlock. Various *N*-substituted piperidines are synthetic intermediates for spermidine nitroimidazole drugs for the treatment of A549 lung carcinoma.<sup>11</sup>

Piperidines have attracted particular attention due to their miscellaneous important activities as pharmacophores in several biologically active compounds, which are responsible for a number of unique activities. So they are widely used in the treatment of cocaine abuse, epileptic disorder, and depression, in the prevention of various inflammatory diseases, immune diseases such as autoimmune diseases or allergic diseases, and HIV infection, and in 5-HT2B receptor antagonists.<sup>12–14</sup> Despite

their great importance, until now there are only a few reports in literature documenting the synthesis of these spiro-substituted compounds.<sup>15–18</sup>

Recently, only two reports on the synthesis of various bis-spiro piperidine have used  $\text{FeCl}_3$  and  $\text{In}(\text{OTf})_3$  for spiro hexahydro pyrimidine. Both reports used homogenous catalysts.<sup>19,20</sup> The use of homogenous catalysts has received little attention as an alternative to alleviating some of the limitations.<sup>21</sup> Thus, the search for an inexpensive, readily available, and convenient catalyst is desirable. The usage of heterogeneous catalysts instead of traditional homogeneous metal Lewis and Brønsted acid catalysts could possess a more environmentally friendly alternative. Development of environmentally friendly solid catalysts for the synthesis of fine chemicals and pharmaceuticals is becoming an area of growing interest.<sup>22–25</sup> Solid catalysts provide numerous opportunities for their easy handling, enhanced reaction times, greater selectivity, simple workup, and recyclability.<sup>26,27</sup>

Among the three used elements (As, Sb or Bi), only As and Sb form with chloride preclude any coordination chemistry with ligands.<sup>28</sup>  $\text{SbCl}_5$  is a powerful Lewis acid and a strong chlorinating agent, widely used in organic synthesis, and a large number of complexes with O- or N-donor solvents have been reported.<sup>29,30</sup> The handling and the usability of  $\text{SbCl}_5$  in liquid form is laborious and the supported form is indeed preferable. Supported  $\text{SbCl}_5$  on nano  $\gamma$ -alumina has been prepared and used effectively as a catalyst.

Since the ordered mesoporous silica material was first reported in 1992, the interest in this research field has expanded all over the world due to the potential applications of these materials in catalysis and in other realms of chemistry. Compared to silica, alumina is more popular in the catalysis area for its broad applications as industrial catalysts and

<sup>a</sup>Department of Organic Chemistry, Faculty of Chemistry, University of Kashan, Kashan, I. R. Iran. E-mail: bamoniri@kashanu.ac.ir

<sup>b</sup>Department of Organic Chemistry, College of Science, Yazd University, Yazd, I. R. Iran

† Electronic supplementary information (ESI) available. See DOI: <https://doi.org/10.1039/d3ra00448a>



catalyst support employed in petroleum refinement, automobile emission control, and others. With the characteristics of mesoporous materials, such as highly uniform channels, large surface area, narrow pore-size distribution, tunable pore sizes over a wide range, and so on, alumina with a mesostructure should possess much more excellent properties.<sup>31–34</sup>

In the last few years, ultrasonic (US) irradiation-based reactions have attracted much attention under the banner of 'green chemistry' as they tolerate common benefits of both scientific and industrial fields in organic chemistry predominantly in the area of heterocyclic chemistry.<sup>35–37</sup> US irradiation influences induce high pressure and temperatures inside the acoustic cavitation bubbles and also develop mass transference in the liquid.<sup>38</sup> This unique possession of the US strongly affects the chemical reactivity *via* the dissipation of energy. Additionally, US irradiation offers several significant advantages such as being environmentally friendly, involving rapid reaction time, enriched reaction rates, non-hazardous, excellent yields, mild reaction conditions, and simple handling.<sup>39–41</sup>

However, the development of an efficient and eco-friendly procedure that induces heterogeneous catalysts is highly expected for the synthesis of bis-spiro piperidine derivatives under ultrasonic irradiation and the room temperature method. For this purpose, herein, we have developed an eco-friendly and cost-effective protocol in which bis-spiro piperidine derivatives can be synthesized very easily in a very short reaction time using nano- $\gamma$ -Al<sub>2</sub>O<sub>3</sub>/Sb(v) as a Lewis acids catalyst.

## 2. Experimental

### 2.1 Materials and instrumentation

All chemicals were purchased from Fluka and Merck Chemical Company and used without any additional purification. The Fourier transform infrared (FT-IR) spectra of samples were recorded from 400 to 4000 cm<sup>-1</sup> using an FT-IR Magna 550 apparatus using with KBr plates. A Bruker (DRX-400 Avance) NMR was used to record the <sup>1</sup>H-NMR and <sup>13</sup>C-NMR spectra. XRD pattern using Philips Xpert MP diffractometer (Cu K $\alpha$ , radiation,  $k = 0.154056$  nm) was achieved. FESEM was obtained on a Mira Tescan. Transmission electron microscope (TEM) images were collected on a Philips-CM 120-with LaB<sub>6</sub> cathode instrument on an accelerating voltage of 120 kV. The thermal gravimetric analysis (TGA) was performed with the "STA 504" instrument. Energy-dispersive X-ray spectroscopy (EDS) of nano- $\gamma$ -Al<sub>2</sub>O<sub>3</sub>/Sb(v) was measured using the EDS instrument, Phenom pro X Brunauer–Emmett–Teller (BET) surface area analysis of the catalyst was performed using the Micrometrics, Tristar II 3020 analyser.

### 2.2. Preparation of nano- $\gamma$ -Al<sub>2</sub>O<sub>3</sub>

NaOH (600 ml, 1 M), was added drop-wise to a slurry containing Al<sub>2</sub>(SO<sub>4</sub>)<sub>3</sub>·18H<sub>2</sub>O (66 g). The mixture was stirred at room temperature. The resulting suspension was filtered to obtain the white solid Al(OH)<sub>3</sub>. The solids were washed with distilled water until no more sulfate ions were detected in the washings. After that NaOH (100 ml, 1 M) was added to a beaker containing

Al(OH)<sub>3</sub> (20 g) to produce NaAl(OH)<sub>4</sub>. Then PEG 4000 (0.3%) was added to the solution and it was neutralized with HCl (0.1 M), to pH 8 until Al(OH)<sub>3</sub> was produced again.

The obtained precipitate was filtered and washed with distilled water. The as-dried solid was calcined in the furnace at 800 °C for 3 hours through atmospheric air to produce nano- $\gamma$ -Al<sub>2</sub>O<sub>3</sub> powder.

### 2.3 Preparation of nano- $\gamma$ -Al<sub>2</sub>O<sub>3</sub>/Sb(v)

In a nano- $\gamma$ -Al<sub>2</sub>O<sub>3</sub> (1 g) and CH<sub>2</sub>Cl<sub>2</sub> (10 ml), SbCl<sub>5</sub> (0.5 ml) was added dropwise in the well-ventilated hood. The mixture was then continuously stirred for 1 hour at room temperature and the solid catalyst was separated by filtration, washed with CH<sub>2</sub>Cl<sub>2</sub>, and dried at room temperature.

### 2.4 Catalyst characterization

FT-IR spectra of nano- $\gamma$ -Al<sub>2</sub>O<sub>3</sub> (a) and nano- $\gamma$ -Al<sub>2</sub>O<sub>3</sub>/Sb(v) (b) were recorded. In the nano- $\gamma$ -Al<sub>2</sub>O<sub>3</sub> FT-IR spectrum, the band in the region of 500–1000 cm<sup>-1</sup> is attributed to the stretching vibrations of the (Al–O) bond in  $\gamma$ -Al<sub>2</sub>O<sub>3</sub>. In the nano- $\gamma$ -Al<sub>2</sub>O<sub>3</sub>/Sb(v) spectrum, due to the binding of SbCl<sub>5</sub> with  $\gamma$ -Al<sub>2</sub>O<sub>3</sub> two additional bands at 701 cm<sup>-1</sup> are presented (Fig. 1).

In the XRD patterns of the catalyst, the signals at 2 $\theta$  equal to 37 (c), 45 (d), and 67 (e) are displayed nano- $\gamma$ -Al<sub>2</sub>O<sub>3</sub> structure. According to the XRD pattern, the two additional signals at 2 $\theta$  equal to 28 (a) and 32 (b), respectively, are shown as the presentation of bonded Sb to nano- $\gamma$ -Al<sub>2</sub>O<sub>3</sub> (Fig. 2).

However, the presence of the anticipated elements in the construction of this catalyst and corroborated support of SbCl<sub>5</sub>

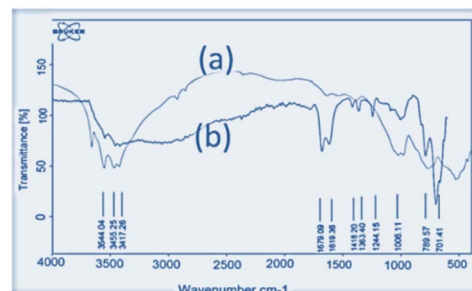


Fig. 1 FT-IR spectra of (a) nano- $\gamma$ -Al<sub>2</sub>O<sub>3</sub> and (b) nano- $\gamma$ -Al<sub>2</sub>O<sub>3</sub>/Sb(v).

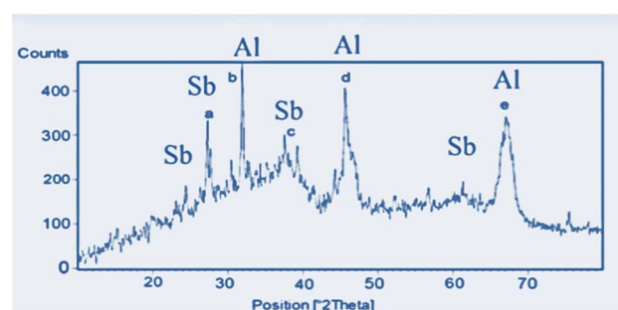
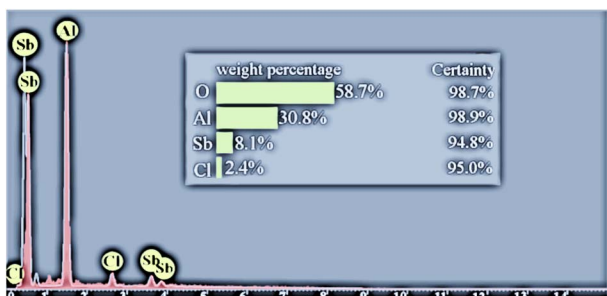
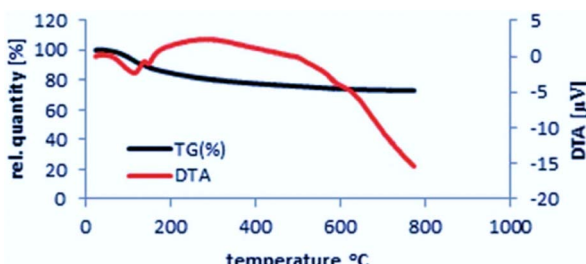


Fig. 2 XRD patterns of nano- $\gamma$ -Al<sub>2</sub>O<sub>3</sub>/Sb(v).

Fig. 3 EDS analysis diagram of nano- $\gamma$ -Al<sub>2</sub>O<sub>3</sub>/Sb(v).Fig. 4 Thermogravimetric analysis (TG-DTA) of nano- $\gamma$ -Al<sub>2</sub>O<sub>3</sub>/Sb(v).

on nano- $\gamma$ -Al<sub>2</sub>O<sub>3</sub> in the catalyst was ascertained by EDS analysis, which showed that the peaks for the presence of the elemental compositions of nano- $\gamma$ -Al<sub>2</sub>O<sub>3</sub>/Sb(v) were found to be 58.7, 30.8 and 8.1% for O, Al, and Sb, respectively (Fig. 3).

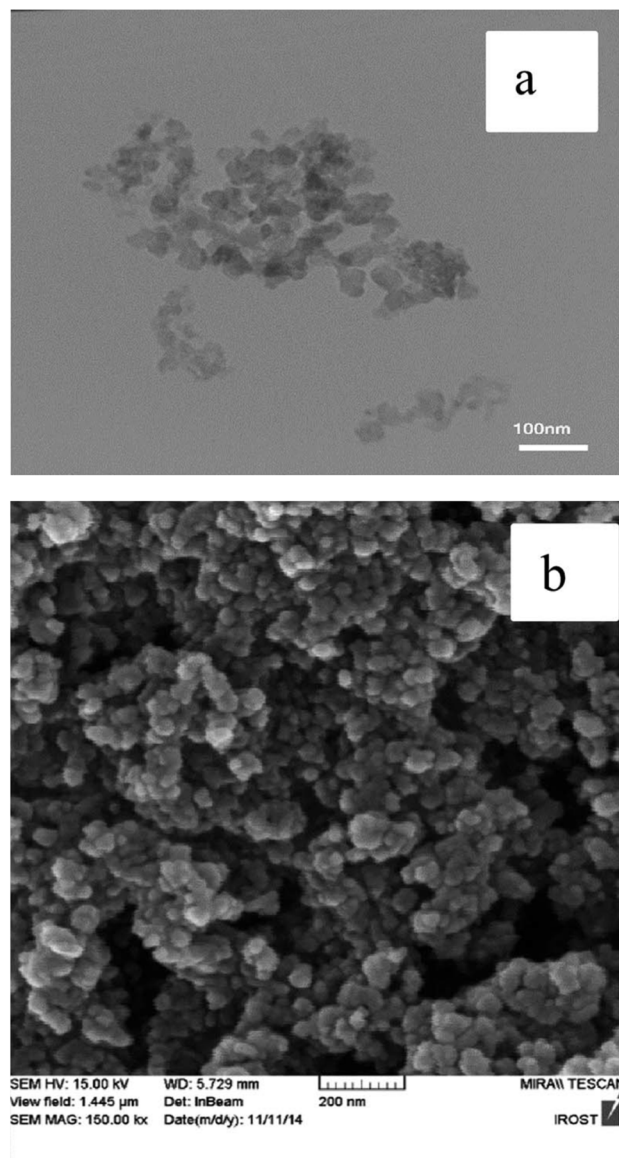
Thermal gravimetric analysis (TG-DTA) was performed in order to evaluate the thermal behavior and stability of the catalyst at elevated temperatures. The pattern of nano- $\gamma$ -Al<sub>2</sub>O<sub>3</sub>/Sb(v) was recorded by heating from 20 °C to 780 °C and then cooling until 165 °C. The catalyst is stable until 390 °C and only 10.5% of its weight was decreased due to the elimination of catalyst humidity. The char yield of the catalyst at 390 °C is 89.5%. According to the TG-DTA pattern of nano- $\gamma$ -Al<sub>2</sub>O<sub>3</sub>/Sb(v) it was revealed that this catalyst is appropriate for the advancement of organic reactions until 400 °C (Fig. 4).

FESEM and TEM images of the nano- $\gamma$ -Al<sub>2</sub>O<sub>3</sub>/Sb(v) confirmed the disordered spherical shape below 50 nm for nanoparticles (Fig. 5).

The BET N<sub>2</sub> adsorption technique was applied to measure the surface area. The BET surface area was 92.503 m<sup>2</sup> g<sup>-1</sup>. The N<sub>2</sub> adsorption isotherm of the catalyst is described. Inductively coupled plasma (ICP) analysis determined the existence 200 mg of Sb in 1 g of the catalyst (Fig. 6).

### 3. Optimization of the reaction conditions

To investigate the feasibility of our protocol for the synthesis of bis-spiro piperidine derivative, a series of experiments were carried out using aniline, dimedone, and formaldehyde in dichloromethane as a model reaction. As various control experiments were performed, first without any catalyst and then

Fig. 5 TEM (a) and FESEM (b) images of nano- $\gamma$ -Al<sub>2</sub>O<sub>3</sub>/Sb(v).

using nano  $\gamma$ -alumina supported SbCl<sub>5</sub> and other Lewis acids such as kaolin-SO<sub>3</sub>H, cellulose-SnCl<sub>4</sub>, SbCl<sub>5</sub>/SiO<sub>2</sub> as catalysts in CH<sub>2</sub>Cl<sub>2</sub> at room temperature (Table 1). The blank experiment without any catalyst and using kaolin-SO<sub>3</sub>H as a catalyst did not show promising catalytic effects (Table 1, entries 1 and 2). Among various Lewis acids, SbCl<sub>5</sub>/SiO<sub>2</sub> showed the most promising catalytic effects (Table 1, entries 4), its ability to be reused led us to explore the use of nano- $\gamma$ -alumina as a support for the SbCl<sub>5</sub>, too. The results obtained were very satisfactory as the product in excellent yield (94%) was obtained in a short time period (Table 1, entry 5). Taking nano- $\gamma$ -alumina supported as the right catalyst for this reaction, the reaction conditions were further optimized by examining the solvent effect on the reaction. Various organic solvents such as dichloromethane, trichloromethane, *n*-hexane, ethanol, acetone, and water were screened to test the efficiency of the catalyst and the results are



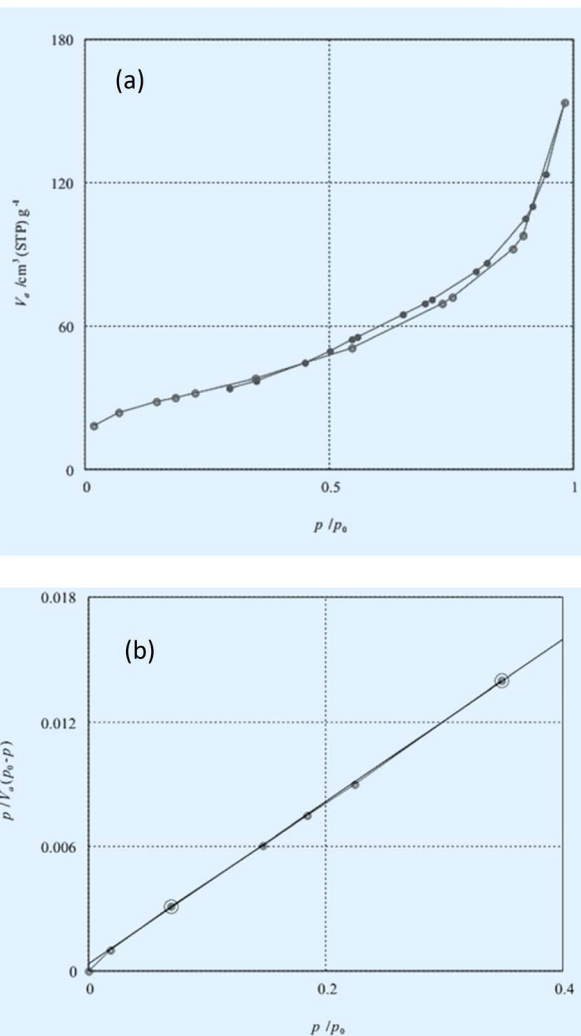


Fig. 6 (a) Nitrogen adsorption/desorption isotherm at 77 K and (b) BET-plot of nano- $\gamma$ -Al<sub>2</sub>O<sub>3</sub>/Sb(v).

summarized in Table 1 (entries 5–10). Meanwhile, the efficiencies of SbCl<sub>5</sub> and Al<sub>2</sub>O<sub>3</sub> in the promotion of the model reaction were examined (entries 11 and 12).

All solvents screened gave low to moderate yields of the product and took a long time period (3–5 h) for the completion of the reaction. In contrast, dichloromethane has shown significant improvement over other solvents in terms of yield and reaction time (Table 1, entry 5).

This rate enhancement of the reaction can be attributed to the unique properties of dichloromethane like hydrogen bonding to stabilize the transition states.

In order to find the optimized amount of the catalyst, the reaction was carried out by varying the amount of the catalyst in the model reaction (Table 2). It was found that the conversion of the bis-spiro piperidine derivative decreased linearly with an increase in the amount of catalyst from 30–100 mg. Further, an increase in the amount of catalyst did not have any profound effect on the reaction. Therefore, 50 mg of nano gamma-alumina supported SbCl<sub>5</sub> was used for the synthesis of bis-spiro piperidines.

Table 1 Effect of different reaction media on model reaction<sup>a</sup>

Entry	Catalyst	Solvent (10 ml)	Time (h)	Yield (%)
1	—	CH <sub>2</sub> Cl <sub>2</sub>	7	0
2	Kaolin-SO <sub>3</sub> H	CH <sub>2</sub> Cl <sub>2</sub>	5	75
3	Cellulose-SnCl <sub>5</sub>	CH <sub>2</sub> Cl <sub>2</sub>	3	84
4	SbCl <sub>n</sub> /SiO <sub>2</sub>	CH <sub>2</sub> Cl <sub>2</sub>	3.30	89
5	Nano- $\gamma$ -Al <sub>2</sub> O <sub>3</sub> /Sb(v)	CH <sub>2</sub> Cl <sub>2</sub>	2.30	94
6	Nano- $\gamma$ -Al <sub>2</sub> O <sub>3</sub> /Sb(v)	CHCl <sub>3</sub>	4	85
7	Nano- $\gamma$ -Al <sub>2</sub> O <sub>3</sub> /Sb(v)	<i>n</i> -Hexane	5	75
8	Nano- $\gamma$ -Al <sub>2</sub> O <sub>3</sub> /Sb(v)	Ethanol	4	80
9	Nano- $\gamma$ -Al <sub>2</sub> O <sub>3</sub> /Sb(v)	Acetone	3.30	75
10	Nano- $\gamma$ -Al <sub>2</sub> O <sub>3</sub> /Sb(v)	Water	5	74
11	Al <sub>2</sub> O <sub>3</sub>	CH <sub>2</sub> Cl <sub>2</sub>	2.30	65
12	SbCl <sub>5</sub>	CH <sub>2</sub> Cl <sub>2</sub>	1	95

<sup>a</sup> The reaction conditions: aniline (1 mmol), dimedone (2 mmol), formaldehyde (3 mmol), catalyst (30 mg), room temperature.

Table 2 Effect of the catalyst (nano- $\gamma$ -Al<sub>2</sub>O<sub>3</sub>/Sb(v)) amount<sup>a</sup>

Entry	Nano- $\gamma$ -Al <sub>2</sub> O <sub>3</sub> /Sb(v) (mg)	Time (h)	Yield (%)
1	30	3	90
2	50	2	98
3	60	3	92
4	80	3	88
5	100	3	86

<sup>a</sup> The reaction conditions: aniline (1 mmol), dimedone (2 mmol), formaldehyde (3 mmol), room temperature.

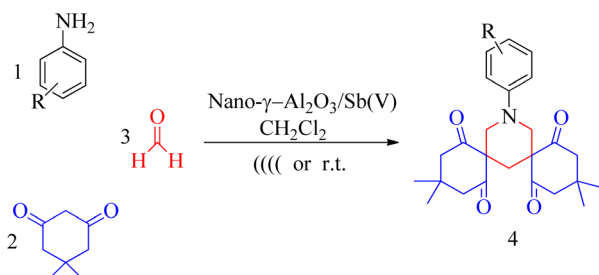
## 4. General procedure for the synthesis of bis-spiro piperidine

The synthesis of bis-spiro piperidines was performed with a reaction of aromatic amine derivatives (1 mmol), dimedone (2 mmol), formaldehyde (3 mmol, 37–41% aqueous solution) in dichloromethane (10 ml) in the presence of nano- $\gamma$ -Al<sub>2</sub>O<sub>3</sub>/Sb(v) (30 mg) under ultrasonic irradiation or room temperature for the required period of times. The appearance of a solid compound denoted the formation of products. After completion of the reaction (monitored by TLC), the resulting products were filtered and recrystallized from ethanol to afford the pure products (Scheme 1).

### 4.1 Optimization of ultrasonic irradiation power

The reaction was examined under various irradiation powers corresponding to 50, 75, 100, 125, and 150 W. When irradiation power was 50 W, a good yield of 75% was seen but lower compared to irradiation at 75 W for 7 min (Table 3, entries 1 and 2). Irradiation at 100 W for 4 min yielded appreciable product yields (Table 3, entry 3). Increase in irradiation power to 125 W procured excellent yields in 2.5 min whereas with further increase in irradiation power, there were no signs of alteration or improvement in yields (Table 3, entries 5). Hence the results approved the optimum ultrasound power for efficient synthesis of bis-spiro piperidine from the multi-component reaction in CH<sub>2</sub>Cl<sub>2</sub> solvent and nano gamma-alumina supported SbCl<sub>5</sub> as catalyst conditions amount to 100 W. The most likely reason behind the positive association of irradiation power with that of





Scheme 1 Synthesis of bis-spiro piperidine derivative.

Table 3 Synthesis of bis-spiro piperidines under US irradiation various frequencies<sup>a</sup>

Entry	Power (W)	Time (min)	Yield <sup>b</sup> (%)
1	50	7	75
2	75	7	80
3	100	4	87
4	125	2.5	95
5	150	2.5	95

<sup>a</sup> 4-Methoxyaniline (1 mmol), dimedone (2 mmol), formaldehyde (37–41%) (3 mmol) and CH<sub>2</sub>Cl<sub>2</sub> (10 ml) in the presence of nano-γ-Al<sub>2</sub>O<sub>3</sub>/Sb(v) (50 mg) and ultrasonic irradiation. <sup>b</sup> Isolated yield.

the reaction improvement is the rise in the population of active cavitation bubbles and the dimension of individual bubbles as well which together result in reaching a maximum in collapse temperature thereby accelerating the reaction.

After modification of conditions, we have compared the catalytic activity of nano-γ-Al<sub>2</sub>O<sub>3</sub>/Sb(v) for the synthesis of bis-spiro piperidine under ultrasonic irradiation at room temperature (Table 4).

## 5. Physical and spectral data of selective compounds

### 5.1 Compound (4f)

mp: 188–190 °C; FTIR (KBr)  $\bar{\nu}$ : 3030, 2922, 1731, 1601–1468, 1350, 1264, 1038 cm<sup>-1</sup>. <sup>1</sup>H NMR (400 MHz, DMSO-d<sub>6</sub>,  $\delta$  ppm): 1.00 (12H, s, CH<sub>3</sub>), 1.72 (2H, s, CH<sub>2</sub>), 2.07 (4H, d,  $^2J_{HH}$  = 17.2 Hz,

CH<sub>2</sub>), 2.23 (4H, d,  $^2J_{HH}$  = 17.2 Hz, CH<sub>2</sub>), 3.33 (3H, s, OCH<sub>3</sub>), 3.66 (4H, s, CH<sub>2</sub>), 6.75 (2H, d,  $^2J_{HH}$  = 7.2 Hz, ArH), 7.05 (2H, d,  $^2J_{HH}$  = 6.4 Hz, ArH).

### 5.2 Compound (4g)

mp: 220–222 °C; FTIR (KBr)  $\bar{\nu}$ : 3030, 2956, 1751, 1677–1418, 1593, 1374, 1263 cm<sup>-1</sup>. <sup>1</sup>H NMR (400 MHz, DMSO-d<sub>6</sub>,  $\delta$  ppm): 0.92 (6H, s, CH<sub>3</sub>), 0.94 (6H, s, CH<sub>3</sub>), 2.61 (2H, s, CH<sub>2</sub>), 2.75 (4H, d,  $^2J_{HH}$  = 13.6 Hz, COCH<sub>2</sub>), 2.85 (4H, d,  $^2J_{HH}$  = 13.6 Hz, COCH<sub>2</sub>), 3.83 (4H, s, NCH<sub>2</sub>), 7.22 (2H, d,  $^3J_{HH}$  = 9.6 Hz, ArH), 8.03 (2H, d,  $^2J_{HH}$  = 9.6 Hz, ArH).

### 5.3 Compound (4h)

mp: 186–188 °C; FTIR (KBr)  $\bar{\nu}$ : 2956, 1751, 1449–1677, 1375–1594, 1264, 767 cm<sup>-1</sup>. <sup>1</sup>H NMR (400 MHz, CDCl<sub>3</sub>,  $\delta$  ppm): 1.03 (6H, s, CH<sub>3</sub>), 1.04 (6H, s, CH<sub>3</sub>), 2.56 (2H, s, CH<sub>2</sub>), 2.69 (4H, d,  $^2J_{HH}$  = 14 Hz, COCH<sub>2</sub>), 2.87 (4H, d,  $^2J_{HH}$  = 14 Hz, COCH<sub>2</sub>), 3.57 (4H, s, NCH<sub>2</sub>), 7.42 (1H, t,  $^2J_{HH}$  = 8 Hz, ArH), 7.59 (2H, dd,  $^2J_{HH}$  = 8.2 Hz, ArH), 7.75 (2H, dd,  $^2J_{HH}$  = 11.8 Hz, ArH).

## 6. Catalyst recycling

From the environmental and economic viewpoints, effective recovery of the catalyst from the reaction mixture is the key factor that determines its utility for practical applications. Thus, catalyst recycling experiments were employed in order to explore the amount of recyclability of our catalytic system. After the completion of the model reaction, the catalyst was recovered by extracting the mixture with ethanol followed by filtration.

Table 5 Reusability potential of nano-γ-Al<sub>2</sub>O<sub>3</sub>/Sb(v) catalyst<sup>a</sup>

No. of cycles	Fresh	Run 1	Run 2	Run 3	Run 4	Run 5
Yield (%) <sup>b</sup>	94	92	91	89	87	85
Time (h)	2.5	2.5	2.5	2.45	2.45	2.45

<sup>a</sup> Aniline (1 mmol), dimedone (2 mmol), formaldehyde (3 mmol) and CH<sub>2</sub>Cl<sub>2</sub> (10 ml) in the presence of nano-γ-Al<sub>2</sub>O<sub>3</sub>/Sb(v) (50 mg).

<sup>b</sup> Isolated yield.

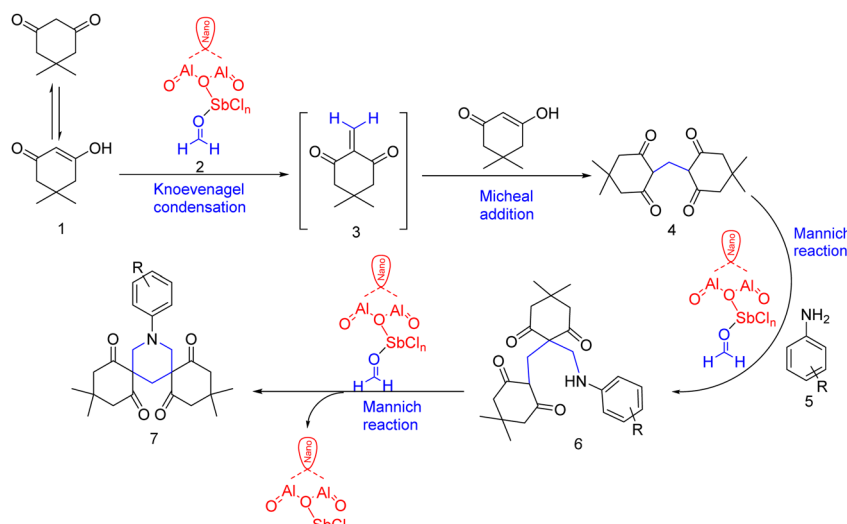
Table 4 Synthesis of bis-spiro piperidine derivatives in the presence of nano-γ-Al<sub>2</sub>O<sub>3</sub>/Sb(v) under sonication or room temperature conditions<sup>a</sup>

Entry	R	Product	Sonication		Room temperature	
			Time (min)	Yield <sup>b</sup> (%)	Time (min)	Yield <sup>b</sup> (%)
1	4-Br	<b>4a</b>	2.5	93	150	93
2	4-Cl	<b>4b</b>	2	94	150	94
3	3,4-Cl	<b>4c</b>	4	89	240	89
4	4-CH <sub>3</sub>	<b>4d</b>	2	90	140	90
5	3-CH <sub>3</sub>	<b>4e</b>	4	87	240	87
6	4-OCH <sub>3</sub>	<b>4f</b>	2	97	160	95
7	4-NO <sub>2</sub>	<b>4g</b>	6.5	81	360	78
8	3-NO <sub>2</sub>	<b>4h</b>	5	97	300	95
9	4-F	<b>4i</b>	3	89	180	82

<sup>a</sup> Aniline derivatives (1 mmol), dimedone (2 mmol), formaldehyde (3 mmol), and CH<sub>2</sub>Cl<sub>2</sub> (10 ml) in the presence of nano-γ-Al<sub>2</sub>O<sub>3</sub>/Sb(v) (50 mg).

<sup>b</sup> Isolated yield.





Scheme 2 Possible reaction mechanism for the synthesis of bis-spiro piperidine derivative.

The catalyst was then washed with ethanol and reused for subsequent cycles. The catalyst activity remained after five runs in a high percentage (Table 5).

## 7. Reaction mechanism

The probable reaction mechanism of synthesis of bis-spiro piperidine was proposed on the basis of reported literature and is outlined in Scheme 2.<sup>42,43</sup> The spirocyclization may be accomplished as a domino progression of Knoevenagel, Michael, and double Mannich reactions. A literature review proved that dimedone is not only a Knoevenagel reagent but it also adds easily to electron-poor alkenes in the Michael addition manner leading to the dimedone formaldehyde adducts 4.<sup>44,45</sup> The famous dimedone formaldehyde adducts then undergo two consecutive Mannich reactions with aromatic amine and formaldehyde to produce the bis-spiro substituted piperidine. Again 4 was also formed by the reaction of dimedone (2 mmol) and formaldehyde (1 mmol) at room temperature in the presence of nano  $\gamma$ -alumina supported  $\text{SbCl}_5$  catalyst. This compound 4 when reacted with aromatic amine afforded the final product 7 (Scheme 2).

## 8. Conclusion

In summary, we synthesized a new solid acid catalyst, nano  $\gamma$ -alumina supported  $\text{SbCl}_5$ , and used it for the green and energy-sustainable synthesis of bis-spiro piperidine derivatives in both ultrasonic irradiation and room temperature. Short reaction times, high conversions, clean reaction profiles, simple work-up, non-hazardous, excellent yields, availability, and high activity of the catalyst, make this method suitable for many acid catalysed organic reactions. The catalyst was found to be highly efficient and could be reused for six catalytic cycles. The use of heterogeneous catalysts under ultrasonic irradiation makes this

protocol environmentally friendly and an energy-sustainable alternative to reported methods.

## Conflicts of interest

There are no conflicts to declare.

## Acknowledgements

The authors are grateful to University of Kashan for financial support of this work.

## References

- 1 B. M. Trost, *Science*, 1991, **55**, 1471–1477.
- 2 J. Collins, *J. Chem. Educ.*, 1995, **72**, 965–970.
- 3 C. Hulme, M. Ayaz, G. Martinez-Ariza, F. Medda and A. Shaw, Recent Advances in Multicomponent Reaction Chemistry, in *Small Molecule Medicinal Chemistry: Strategies and Technologies*, ed. W. Czechtizky and P. Hamley, Wiley & Sons, Inc, New Jersey, 2015, pp. 965–970.
- 4 A. Dömling and A. D. Alqahtani, General Introduction to MCR-s: Past, Present, and Future, in *Multicomponent Reactions in Organic Synthesis*, ed. J. Zhu, Q. Wang and M.-X. Wang, Wiley-VCH Verlag GmbH & Co. KGaA, Weinheim, Germany, 2014, pp. 1–43.
- 5 B. H. Rotstein, S. Zaretsky, V. Rai and A. K. Yudin, *Chem. Rev.*, 2014, **114**, 8323–8359.
- 6 H. Bienaymé, C. Hulme, G. Oddon and P. Schmitt, *Chem. – Eur. J.*, 2000, **6**, 3321–3329.
- 7 I. Ugi, *Pure Appl. Chem.*, 2001, **73**, 187–191.
- 8 R. Saul, J. P. Chambers, R. J. Molyneux and A. D. Elbein, *Arch. Biochem. Biophys.*, 1983, **2**, 593–597.
- 9 D. O'Hagan, *Nat. Prod. Rep.*, 2000, **17**, 435.
- 10 J. W. Daly, T. F. Spande and H. M. Garraffo, *J. Nat. Prod.*, 2005, **68**, 1556.



11 A. Q. Siddiqui, L. Merson-Davies and P. M. Cullis, *J. Chem. Soc., Perkin Trans. 1*, 1999, 3243.

12 H. Bienayme, L. Chene, S. Grisoni, A. Grondin, B. Kaloun, S. Poigny, H. Rahali and E. Tam, *Bioorg. Med. Chem. Lett.*, 2006, **16**, 4830.

13 C. A. Maier and B. Wunsch, *J. Med. Chem.*, 2002, **45**, 438.

14 V. V. Rostovtsev, L. G. Green, V. V. Fokin and K. B. Sharpless, *Angew. Chem.*, 2002, **114**, 2708.

15 N. G. Kozlov and A. P. Kadutskii, *Tetrahedron Lett.*, 2008, **49**, 4560.

16 C. Jr Viegas, V. S. Da Bolzani, M. Furlan, E. J. Barreiro, M. C. M. Young, D. Tomazela and M. N. Eberlin, *J. Nat. Prod.*, 2004, **67**, 908.

17 P. M. Dewick, *Medicinal Natural Products: A Biosynthetic Approach*, Wiley, New York, 2nd edn, 2002, p. 307.

18 S. Petit, J. P. Nallet, M. Guillard, J. Dreux, M. P. Chermat, C. Bulach, P. Simon, C. Fontaine, M. Barthelmebs and J. L. Imbs, *Eur. J. Med. Chem.*, 1991, **26**, 19.

19 C. Mukhopadhyay, S. Rana and R. J. Butcher, *Tetrahedron Lett.*, 2011, **52**, 4153–4157.

20 A. Dandia, K. A. Jain and S. Sharma, *Tetrahedron Lett.*, 2012, **53**, 5270.

21 G. N. Kozlov and P. A. Kadutskii, *Tetrahedron Lett.*, 2008, **49**, 4560.

22 P. S. Andrews, F. A. Stepan, H. Tanaka, V. S. Ley and D. M. Smith, *Adv. Synth. Catal.*, 2005, **347**, 647.

23 T. Miao and L. Wang, *Tetrahedron Lett.*, 2007, **48**, 95.

24 M. A. Trzeciak, E. Mieczynska, J. J. Ziolkowski, W. Bukowski, A. Bukowska, J. Noworol and J. Okal, *New J. Chem.*, 2008, **32**, 1124.

25 X. Ma, Y. Zhou, J. Zhang, A. Zhu, T. Jiang and B. Han, *Green Chem.*, 2008, **10**, 59.

26 K. J. Ratnam, R. S. Reddy, N. S. Sekhar, M. L. Kantam, A. Deshpande and F. Figueras, *Appl. Catal., A*, 2008, **348**, 26.

27 M. Abid, M. Savolainen, S. Landge, J. Hu, G. K. Surya Prakash, G. A. Olah and B. Török, *J. Fluorine Chem.*, 2007, **128**, 587.

28 S. Haupt, K. Seppelt and Z. Anorg, *Z. Anorg. Allg. Chem.*, 2002, **628**, 729.

29 M. Webster, *Chem. Rev.*, 1965, **65**, 87.

30 J.-E. Kessler, C. T. G. Knight and A. E. Merbach, *Inorg. Chim. Acta*, 1986, **115**, 75.

31 C. T. Kresge, M. E. Leonowicz, W. J. Roth, J. C. Vartuli and J. S. Beck, *Nature*, 1992, **359**, 710.

32 J. S. Beck, J. C. Vartuli, W. J. Roth, M. E. Leonowicz, C. T. Kresge, K. D. Schmitt, C. T.-W. Chu, D. H. Olson, E. W. Sheppard, S. B. McCullen, J. B. Higgins and J. L. Schlenkert, *J. Am. Chem. Soc.*, 1992, **114**, 10834.

33 S. E. Tung and E. J. McIninch, *Catal.*, 1964, **3**, 229.

34 H. Topsoe, B. S. Clausen and F. E. Massoth, *Hydrotreating Catalysis*, Springer, Berlin, 1996, p. 310.

35 S. Maddila, S. Gorle, S. Shabalala, O. Oyetade, S. N. Maddila, P. Lavanya and S. B. Jonnalagadda, *Arabian J. Chem.*, 2019, **12**, 671–679.

36 N. Shabalala, N. Kerru, S. Maddila, W. E. van Zyl and S. B. Jonnalagadda, *Chem. Data Collect.*, 2020, **26**, 100365.

37 S. N. Maddila, S. Maddila, M. Khumalo, S. V. H. S. Bhaskaruni and S. B. Jonnalagadda, *J. Mol. Struct.*, 2019, **1185**, 357–360.

38 N. Shabalala, S. Maddila and S. B. Jonnalagadda, *Res. Chem. Intermed.*, 2016, **42**, 8097–8108.

39 R. Pagadala, S. Maddila and S. B. Jonnalagadda, *Green Chem. Lett. Rev.*, 2014, **7**, 131–136.

40 R. Pagadala, S. Maddila and S. B. Jonnalagadda, *Ultrason. Sonochem.*, 2014, **21**, 472–477.

41 N. Kerru, S. Maddila and S. B. Jonnalagadda, *Curr. Org. Chem.*, 2019, **23**, 3156–3192.

42 C. Mukhopadhyay, S. Rana and R. J. Butcher, *Tetrahedron Lett.*, 2011, **52**, 4153.

43 A. Dandia, A. K. Jain and S. Sharma, *Tetrahedron Lett.*, 2012, **53**, 5270.

44 S. Ray, M. Brown, A. Bhaumik, A. Dutta and C. Mukhopadhyay, *Green Chem.*, 2013, **15**, 1910.

45 M. Li, C. Chen, F. He and Y. Gu, *Adv. Synth. Catal.*, 2010, **352**, 519.

